Self-similarity in particle laden flows at constant volume

Natalie Grunewald
Institut für Angewandte Mathematik, Universität Bonn, Wegelerstr. 10, 53115 Bonn, Germany, grunewald@iam.uni-bonn.de

Rachel Levy
Department of Mathematics, Harvey Mudd College, 301 Platt Blvd., Claremont, CA 91711, levy@hmc.edu

Matthew Mata
Department of Mathematics, University of California Los Angeles, 520 Portola Plaza, Los Angeles, CA 90095-1555, matthewmata@math.ucla.edu

Thomas Ward
Department of Mechanical and Aerospace Engineering, North Carolina State University, Raleigh, NC 27695-7910, tward@ncsu.edu

Andrea L. Bertozzi
Department of Mathematics, University of California Los Angeles, 520 Portola Plaza, Los Angeles, CA 90095-1555, bertozzi@math.ucla.edu

December 22, 2008

Abstract. We consider constant volume thin film slurries on an incline. Clear fluids in this geometry are known to have a front position that moves according to a $t^{1/3}$ scaling law, based on similarity solution analysis [Huppert, Nature, 1982]. We investigate the same dynamics for particle laden flow using a recently proposed lubrication model for the slurry and physical experiments. Our analysis includes the role of a precursor in the model. We conclude that in the lubrication model, the height of the precursor significantly influences the speed of the fluid front, independent of particles settling in the direction of flow. By comparing theory with experiments we conclude that the $t^{1/3}$ scaling law persists, to leading order, for slurry flows with particle settling. However additional physics is needed in the existing lubrication models to quantitatively explain departures from clear-fluid self-similarity due to particle settling.

Keywords: Particle laden film, thin liquid films, sedimentation, Riemann problems, systems of conservation laws, gravity driven film flow, self-similarity

1. Introduction

The modeling of gravity-driven particle-laden flows, known as slurries, is of interest in the context of geological phenomena such as mudslides and industrial applications, such as food science (Monquet et al, 2006; Rao et al, 2002). This paper compares the behavior of a constant mass slurry flow down an incline with a pure fluid flow. We compare the analytical solutions of the pure fluid flow to both physical experiments and numerical simulations of the slurry flow, using a model proposed in (Cook et al., 2007/08; Zhou et al., 2005).

In (Huppert, 1982) a simple scaling law is derived for the average front position $x(t) \sim C \cdot t^{1/3}$ in the case of clear fluids. Comparison to both the slurry lubrication model and to physical experiments suggest that the Huppert scaling law is still valid to leading order for slurries with moderate particle concentrations in the range 30-55%. In this range, the slurry still behaves fluid-like, and settling of the particles is present but does not dominate the large scale dynamics. The effects of settling in the direction of the flow can be visually observed in the experiments as a particle-rich ridge at the leading edge of the slurry. We compare different settling functions in our model to analyze this effect numerically. We also note that the lubrication models with settling require a precursor; they are singular at vanishing precursor (Zhou et al., 2005; Cook et al., 2007/08). Thus it makes sense to compare the dynamics of the lubrication model with settling to an exact solution of the problem without settling and with precusor.

The paper is organized as follows: Section 2 reviews the slurry lubrication model to be used here for numerical simulations. Section 3 rederives the original Huppert solution with the addition of a precursor layer in the model. This necessitates a more careful assessment of shock dynamics not present in the original Huppert derivation. Section 4 presents experimental results with heavy particles and Section 5 presents numerical results of the lubrication model with settling and comparison to both the clear fluid model and to experiments.

2. A lubrication model for particle-laden flow

The flow of a particle-laden fluid down an inclined plane has recently been modeled by a system of scalar conservation laws (Cook et al., 2007/08; Cook, 2007),

$$\frac{\partial h}{\partial t} + \nabla \cdot (h v_{tot}) \; = \; 0, \tag{1}$$

$$\frac{\partial(\phi h)}{\partial t} + \nabla \cdot (\phi h v_p) \;=\; 0. \tag{2}$$

The total mass of the fluid is conserved in (1), where $h(x,t)$ is the height of the fluid-particle mixture at time t and position x (oriented down the substrate). The total amount of particles ϕh is conserved in (2), where ϕ is the volume concentration of particles in the fluid. The total velocity of the mixture v_{tot} is a volume average of the speeds of the fluid and the particles. The velocity of the particles v_p consists of the fluid speed v_{tot} and an extra term due to the sedimentation of the more dense particles in the fluid:

$$v_p = v_{tot} + (1-\phi)\, v_{rel}.$$

The depth-averaged velocity of the fluid, v_{tot} found in (1), can be derived via standard techniques in lubrication theory for thin liquid films (Cook, 2007), which is valid for fluids with small Reynolds numbers and characteristic height much smaller than the characteristic length. The first order term describes its dominant behavior as:

$$v_{tot} \;=\; \frac{h^2}{3\mu(\phi)}\, \rho(\phi)\, g_{\|}. \tag{3}$$

While the derivation is standard, it should be noted that the fluid viscosity $\mu(\phi)$ and density $\rho(\phi)$ are both functions of the particle concentration. Following the modeling suggested in (Krieger, 1972; Stickel and Powell, 2005), we model the viscosity with the empirically derived model

$$\mu(\phi) = \mu_f (1 - \phi/\phi_m)^{-2}$$

with dynamic fluid viscosity μ_f. The random packing fraction of spheres ϕ_m is the maximum possible concentration of spheres in a fluid. The density is a linear combination of the density of the fluid ρ_f and the density of the particles ρ_p

$$\rho(\phi) = \rho_f(1-\phi) + \rho_p \phi.$$

The other constant in (3) is the component of gravitational acceleration $g_{\|} = |g| \sin\theta$, where θ is the inclination angle of the substrate.

The velocity v_p in the second conservation law (2) requires more explicit description, since the theory for particle-laden flow is still relatively novel and continues to present many open questions, especially for shear-driven flows. Recall that the lubrication approximation used to derive (3), employs a depth-averaged velocity. We also employ a

depth-averaged model for v_{rel}, which we assume is a product of three factors:

$$v_{rel} \;=\; v_s\, f(\phi)\, w(h), \tag{4}$$

The Stokes settling velocity v_s is the speed at which a single particle with diameter d will settle in a fluid of a given viscosity and density:

$$v_s = \frac{2}{9}\frac{(\rho_p - \rho_f) g_{\|} (d/2)^2}{\mu_f}.$$

The other factors account for phenomena that reduce the speed of a single particle: hindered settling from adjacent particles and slowing due to proximity of particles to the substrate, see also (Taylor, film).

A classical model for hindered settling was proposed by Richardson and Zaki (Richardson and Zaki, 1954) and Buscall (Buscall et al., 1982):

$$f(\phi) = \left(1 - \frac{\phi}{\phi_m}\right)^{\alpha} \tag{5}$$

with $\phi_m = 1$ and empirically determined exponent $\alpha = 5.1$. Cook et al (Cook, 2007) modified the function to include the maximum packing fraction of particles $\phi_m = 0.67$ to avoid singular shocks in solutions to the Riemann problem for (1) and (2) that occur when $\phi_m = 1$. This form also ensures that sedimentation stops once the maximum concentration is reached. We will compare results for $\alpha = 1$ and $\alpha = 5$ to probe the effect of the exponent in the hindered settling function. This is particularly relevant when comparing numerical results and physical experiments, since the division by the maximum packing fraction may have altered the appropriate choice of exponent for comparison to experiments. Note that although the singular limits for both functions

$$\lim_{\phi \to \phi_m} f(\phi) = 0, \qquad \lim_{\phi \to 0} f(\phi) = 1,$$

are appropriate, we will not consider extreme values of ϕ, since the comparison to experiments is most appropriate for moderate concentrations of particles.

The third factor in (4) models the slowing of particles due to their proximity to the substrate, sometimes called the wall effect (Zhou et al., 2005) and (Cook, 2007)

$$w(h) = \frac{\frac{1}{18}(h/d)^2}{\sqrt{1 + \left[\frac{1}{18}(h/d)^2\right]^2}}.$$

Note that $w(h)$ is close to 0 for $h \ll d$ and close to 1 for $h \gg d$. The full system of equations for $h(x,t)$ and $\phi(x,t)$ is now fully specified by incorporating (3) into (1) and (4) into (2).

As has been shown for clear fluids (Bertozzi and Brenner, 1997) a first order model such as the one proposed here can correctly capture quatities such as front speed but does not contain the physics necessary to model fingering due to surface tension and the normal component of gravity to the substrate. Numerical evidence in (Cook, 2007) for constant flux boundary conditions indicates that higher order terms smooth the solutions but do not affect the speed of the leading front of the film. Nevertheless, quite a lot of information can be gained by studying the dominant physics in the flow direction, in particular with regard to the competition between settling of particles and overall motion of the fluid.

Nondimensionalizing the reduced system with length scale h_0 (half of the upstream gate height) and timescale $t_0 = \sin\theta\ t$ we obtain

$$\partial_t h + \partial_x \left(\frac{g\,\rho(\phi)}{3\,\mu(\phi)} h^3 \right) = 0, \tag{6}$$

$$\partial_t(h\phi) + \partial_x \left(\frac{g\,\rho(\phi)}{3\,\mu(\phi)} \phi h^3 + v_s \phi h (1-\phi) f(\phi) w(h) \right) = 0, \tag{7}$$

which we solve numerically and compare to experimental results. Note that this system has been studied in (Cook, 2007) for constant flux boundary conditions. Since the physical experiment (described in section 4) more closely resembles a constant volume of slurry than a constant flux, we will choose initial conditions to approximate a constant volume of fluid for the purpose of numerical simulations.

3. Pure fluid similarity theory including precursor

We begin our discussion of similarity solutions by considering a model for fluid flow without particles, down an incline. Since the density and viscosity for the particle model depend on the particle concentration, we compute numerical simulations for clear fluid flow with density and viscosity matched to the initial concentration of the slurry flow. We measure the effect of the addition of particles to the flow by comparing it to the motion of a pure fluid flow:

$$h_t + \frac{g\,\rho}{3\,\mu} \left(h^3 \right)_x = 0. \tag{8}$$

This model from (Huppert, 1982) captures the dominant behavior of the flow with no particles. For simulations with no precursor, the solu-

tion of (8) for an initial fluid profile

$$h_0(x) = \begin{cases} \beta & \text{if } x \in [0,a] \\ 0 & \text{else} \end{cases}$$

can be solved explicitly. After an initial transient time $t \geq t^* = \frac{3\,a\,\mu}{2\,\beta^2\,g\,\rho}$ a similarity solution

$$h(t,x) = \begin{cases} (\frac{\mu}{g\,\rho})^{1/2}\,\sqrt{x/t} & \text{if } x \in [0, x_s(t)] \\ 0 & \text{else} \end{cases}$$

develops with

$$x_s(t) = \left(\frac{3}{2}\,\beta\,a\right)^{2/3}\,\left(\frac{g\,\rho}{\mu}\right)^{1/3}\,t^{1/3} = C\,\cdot\,t^{1/3},$$

where

$$C = \left(\frac{3}{2}\right)^{2/3}\,\beta^{2/3}\,a^{2/3}\,\left(\frac{g\,\rho}{\mu}\right)^{1/3}. \tag{9}$$

The constant C, when measured experimentally, provides a method for measuring the effective viscosity of the fluid by inverting (9)

$$\mu = \frac{9}{4}\,\beta^2\,a^2\,g\,\rho\,C^{-3}.$$

The effectiveness of this quantity as a measure for bulk viscosity of the slurry is explored in (Ward et al., 2008). For comparison between numerical experiments and simulations, we focus on the variation in the scaling constant C for experiments with and without particles.

It is also possible to consider analytical solutions of (8) with a small uniform precursor layer of height b. For simplicity, let us rescale time by setting $\tau = \frac{g\rho}{\mu}t$ and consider (8) with Riemann initial data

$$u_0(x) = \begin{cases} \beta & \text{if } x \in [0,a], \\ b & \text{else.} \end{cases}$$

The discontinuity in the initial data at $x = 0$ will immediately become a rarefaction, while the shock at $x = a$ will persist. At a critical time

$$\tau_c = \frac{a}{\beta^2 - \frac{1}{3}(\beta^2 + \beta\,b + b^2)},$$

the trailing rarefaction and leading shock will merge, creating a wedge shape that continues to evolve in time above the precursor. The shape of this profile can be described analytically (Lax, 1973; Evans, 1998).

The speed of the leading shock varies in time as does its height. Since the shape of the rarefaction is a squareroot one can use conservation of mass to determine the speed of the shock. Let x_s be the position of the shock. The area under the rarefaction and above the precursor is constant in time, and can be expressed as

$$\int_{b^2\tau}^{x_s} \sqrt{x/\tau}\, dx \; - \; b\,(x_s - b^2\tau) = a\,(\beta - b)$$

by equating the area of the evolving shape to the area of the initial data. Therefore the shock position is defined implicitly by the solution of

$$\frac{2}{3}\,(x_s\sqrt{x_s/\tau} - b^3\tau) \; - \; b\,(x_s - b^2\tau) \; - \; a\,(\beta - b) \; = \; 0 \tag{10}$$

and the solution of the double Riemann problem with precursor after $t = t_c$ is

$$u(x,t) = \begin{cases} b & x < \frac{b^2 g\rho}{\mu} t, \\ \left(\frac{\mu}{g\rho}\right)^{1/2} \sqrt{\frac{x}{t}} & \frac{b^2 g\rho}{\mu} t < x < x_s, \\ b & x > x_s. \end{cases} \tag{11}$$

Figure 1 illustrates the dependence of the evolution of the front position on the height of the precursor.

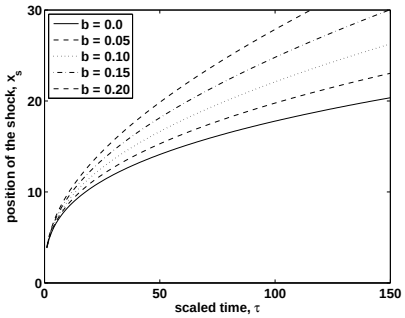

Figure 1. Comparison of front position for different precursor heights

To explore the difference in evolution of the solutions analytically, let

$$\frac{x}{\tau^{1/3}} = Y$$

and substitute for x in (10). In the resulting equation,

$$\frac{2}{3}Y^{2/3} - a\beta + \frac{1}{3}b^3\tau - b\tau^{1/3}Y + ab = 0,$$

the first two terms persist for the solution with no precursor, $b = 0$. The last three terms are responsible for the deviation between the solutions evident in Fig. 1. The last term is constant, which would indicate a deviation between the solutions even at time zero, but recall that there is a different transient for $b = 0$ and $b > 0$, so extrapolation back to zero is not meaningful.

4. Experimental Results

The experimental apparatus consists of a 100 cm long, 50 cm wide acrylic sheet mounted to an adjustable stand capable of inclination angles ranging from 5° to 80°. Down the length of the substrate is a track approximately 14 cm wide and side walls, approximately 3.2 cm high near the top and 1.4 cm lower on the track, designed so the fluid does not escape over the sides. Near the top of the acrylic sheet is a gated reservoir from which a finite well-mixed volume of fluid-particle slurry is released.

The experiments shown are all conducted at an inclination angle of 45 degrees and particle concentrations of 25% to 45%, in increments of 5%. For these values we avoid the rapid settling of the particles toward the substrate associated with low concentrations and low inclination angles which leads to deposits of particles at the rear of the flow and clear fluid fingers at the leading edge. We also avoid particle jamming, clumping and sliding that is associated with higher particle concentrations and higher inclination angles. Additional experimental data have been collected for other inclination angles (Ward et al., 2008); but the data presented here for 45 degrees provide representative results.

The slurry solution is a mixture of 1000 cSt silicone oil (Clearco Products) with a density of approximately 0.96 g/cm^3, and soda-lime glass beads (Ceroglass) with a density of approximately 2.5 g/cm^3. The diameter of the beads is approximately 0.025 cm. For smaller particles, the settling in the direction of the flow to form a particle ridge at the front is less evident.

The maximum packing fraction of beads is determined experimentally as described in (Ward et al., 2008). The value of ϕ_m is measured to be approximately $0.57-0.58$ which is within 15% of the theoretically predicted value of 0.67 for monodisperse hard spheres (we note that our spheres are not perfectly monodisperse). Each preparation of slurry has a constant volume of 90 cm^3 with approximately 70 cm^3 actually being transferred from the jar into the reservoir.

To begin the experiment, the slurry materials are placed in a plastic container and hand mixed using a stirring rod for 4 minutes, creat-

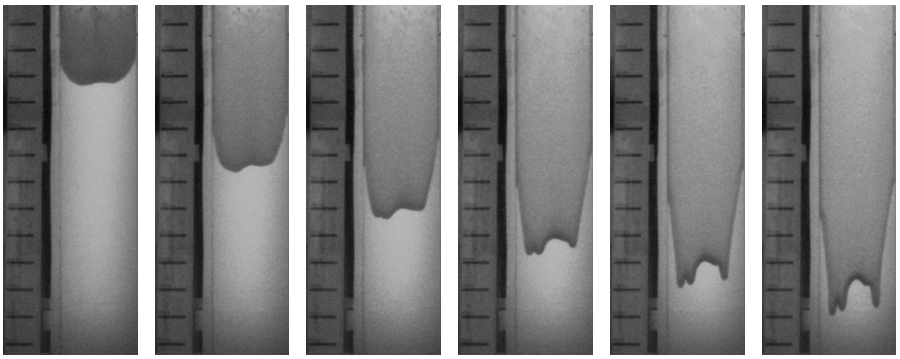

Figure 2. Time series 45 seconds apart, 35 percent concentration, 45 degree inclination.

ing a well-mixed slurry. Since the density of the particles is greater than that of the fluid, the particles settle out fairly quickly and the experiments must be performed immediately after the slurry is well-mixed. The slurry is placed in the reservoir and the gate is opened. A camera positioned above the track and perpendicular to the substrate records still images at predetermined time intervals. The images for the 25% and 30% particle concentration experiments are recorded at 4 fps (frames per second), the 35% and 40% at 2 fps, and the 45% at 1 fps.

The images are analyzed by an image processing code and an average front position is calculated for each image. Figure 2 shows a time-series of images taken at 45 second intervals. In these images the development of the fingering instability and a dark particle-rich ridge at the front of the slurry can be observed. Figure 3 contains a series of plots each taken two minutes into the experiment for a range of particle concentrations. Note that the slurries with more particles move more slowly, and have a darker particle ridge at the front.

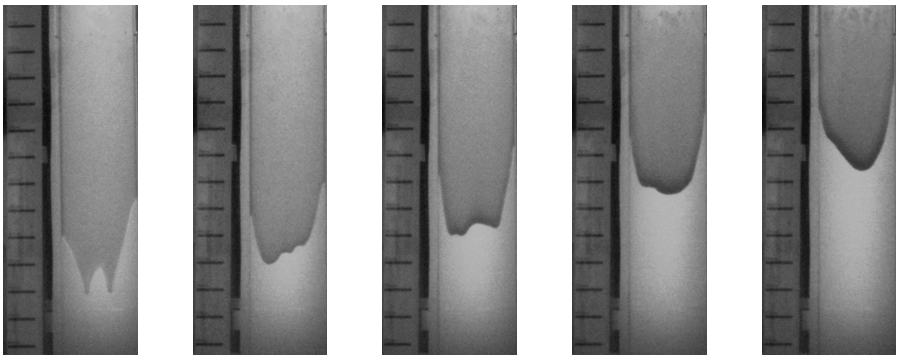

Figure 3. Varying concentrations $25, 30, 35, 40$ and 45 percent at 2 minutes.

The images recorded by the camera are processed to extract the profile of the leading edge of the fluid. A front position for the central half of the flow (away from the side walls), measured in pixels and averaged over approximately 125 data points, is calculated and later converted into a physical distance. The average front position (cm) is plotted against time (s) (rescaled by the inclination angle) to the one-third power in Figure 4. After an initial transient, the data is approximately linear with slope (found using least squares) analogous to the scaling constant C of (9), which decreases with increasing particle concentration.

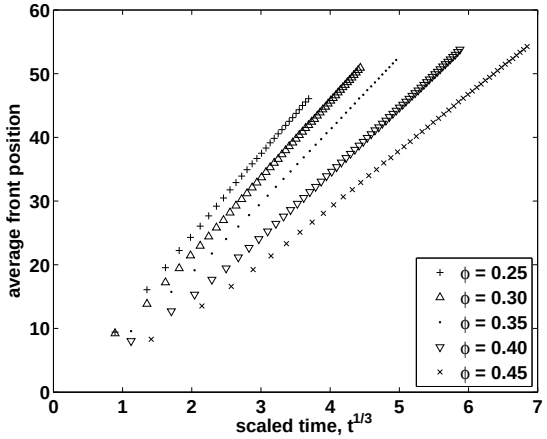

Figure 4. Experimental results tracking the average front position and plotting it against time $t^{1/3}$.

5. Numerical simulations

In this section we describe numerical simulations for the model of a particle-laden film with settling, i.e. (6) and (7). This model requires a precursor as it has been shown that solutions with settling depend singularly on the precursor thickness (Zhou et al., 2005; Cook et al., 2007/08). The simulations employ an upwind finite difference scheme, which is efficient for conservation laws with a unidirectional velocity. We use the experimental parameters described in section 4 and initial data of the step-like form described in section 3. The initial particle concentration is uniform, representing the well-mixed initial slurry in the physical experiment.

We compute solutions with settling function (5) for $\alpha = 1$ and $\alpha = 5$. Recall that the value for the exponent α that was determined

experimentally, (Richardson and Zaki, 1954). For each of the settling functions, Figure 5 contains snapshots in time of numerical solutions of (7). In the left hand plot which contains solutions using the settling function (5) with $\alpha = 1$, the magnitude of the plots in the vertical direction is larger than solutions using the settling function (5) with $\alpha = 5$. This phenomenon has been described in (Cook et al., 2007/08) as a singular shock. However at these scales, the plots are qualitatively similar. From the modeling point of view the exponent $\alpha = 1$ seems to be more appropriate as it shows a stronger ridge that is also observed experimentally. For $\alpha = 5$ the concentrations vary less than 1%.

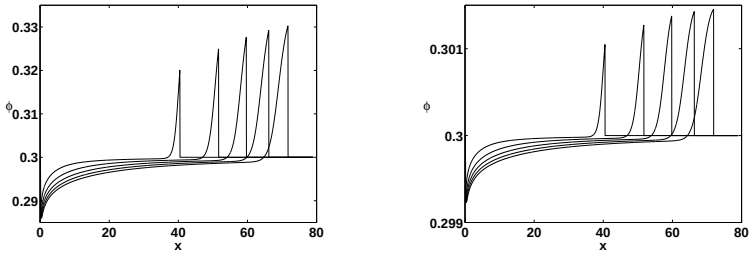

Figure 5. Numerical simulations of particle concentration solutions of (6) and (7) for settling function (5) with $\alpha = 1$ (left) and $\alpha = 5$ (right) at times $t = 30, 60, 90, 120$. While the plots look qualitatively similar, the more singular solutions for $\alpha = 1$ have larger maxima.

In Figure 6, we compare the profile shapes for the analytical solution with precursor (left) and the numerical solution with settling function (5). To compare profile shapes we rescale the data by maximum height in h and by front position in x. We see that the addition of particle settling exhibits departures from pure self-similarity, as seen in the profile shapes, for times relevant to us. Another comparison of the fronts is illustrated in Figure 7. It shows that the height of the precursor makes a much more significant difference in the front speed than the addition of the particle settling. With a precursor, the front speed is similar for both the analytical solution and the settling models of either power and faster than that of the similarity solution with no precursor.

Figure 8 is the numerical version of Figure 4 in the physical experiments. It demonstrates that the dependence of the scaling constant C on the initial concentration has the same trend qualitatively, with slopes C decreasing as the initial concentration ϕ increases.

A quantitative comparison between analytical, numerical and experimental results is provided in Figure 9. The solid line represents the theoretical constants derived from the analytical solutions (without precursor). The numerical values for C for the different settling functions are so similar that the points are virtually indistinguishable

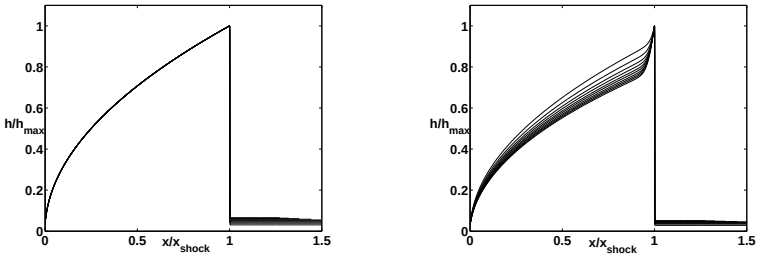

Figure 6. A comparison of scaled solutions. On the left, simulations of (6-7) with precursor but no particle settling. On the right, simulations with precursor and settling with $\alpha = 1$. Both simulations have precursor height 0.05 and initial concentration $\phi = 0.4$.

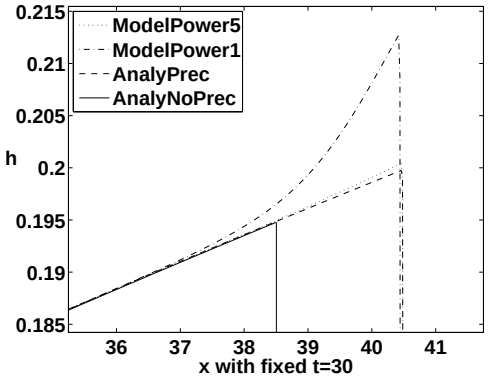

Figure 7. Comparison of solutions to the model (6-7) with analytical solutions (11) of the Riemann problem with and without precursor for initial $\phi = 0.3$.

on this plot and are represented by a single averaged point. The best agreement between the numerical results from the system (6) and (7) and the experimental results is for an initial particle concentration of approximately 0.45. We conjecture that this is a balancing point between low particle concentrations when settling to the substrate is dominant and high particle concentrations when clumping and sliding behavior dominates.

6. Conclusion

We have developed a new understanding of the role of the precursor in lubrication models for thin film slurries, in determining the speed of the front of the slurry. Settling of the particles in the direction of the flow primarily affects the profile of the film as a particle-rich ridge

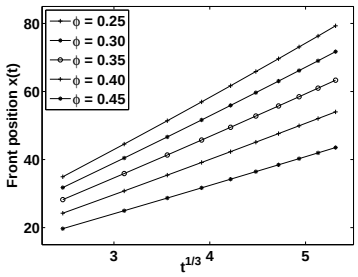

Figure 8. The front position $x(t)$ versus $t^{1/3}$ for different concentrations.

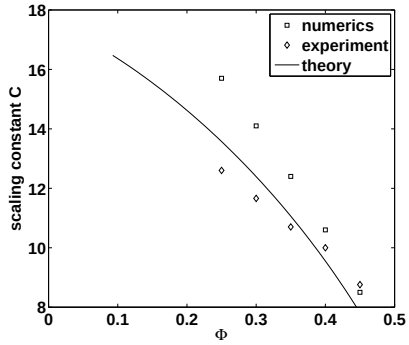

Figure 9. Dependence of scaling constant C on particle concentration ϕ. Note that the numerical data is independent of the choice of settling function.

develops at the front, and has a less significant effect on the speed of the front.

The scaling for the front speed that is exact for analytical solutions with and without precursor is also appropriate to leading order for numerical simulations of the model with particle settling. Both the physical and numerical experiments show the development of a particle rich ridge at the tip of the slurry. However it is also clear that the model does not quantitatively reproduce departure from self-similarity observed in the experiment. A separate paper, on the transverse fingering instability with surface tension (Cook et al, 2009) also suggests that some important physics is missing from the lubrication model, even when surface tension effects are included in the mathematics. One possibility of additional physics to include in this analysis is shear induced migration (e.g. (Leighton and Acrivos, 1986; Leighton and Acrivos, 1987)) which has recently been shown to give quantitatively accurate predictions of phase transitions between settling to the substrate and settling to contact line in constant flow-rate experiments (Cook, 2008).

It would also be interesting to incorporate a precursor into the physical experiments.

The understanding of slurry flows and the relationship to pure fluid and pure granular models is still at a preliminary stage. Appropriate modeling for low concentrations, in which settling to the substrate creates a phase transition in which part of the fluid becomes particle-free needs more modeling. The high particle concentrations that exhibit sliding of large clumps will require yet another (if fluid, then non-Newtonian) model.

Acknowledgements

Natalie Grunewald was supported by the DFG grant GR 3391/1-1. She thanks Andrea Bertozzi and UCLA for their kind hospitality during the last year. This work was supported by ONR grant N000140610059, and NSF grants ACI-0321917, DMS-0601395, and DMS-0502315. We thank Ben Cook and A. E. Hosoi for helpful discussions.

References

Monquet, C., Greffeuille, V. and Treche, S. Characterization of the consistency of gruels consumed by infants in developing countries: assessment of the Bostwick consistometer and comparison with viscosity measurements and sensory perception. *Int. J. Food. Sci. Nutr.*, 57, 459, 2006.

Rao, R., Mondy,L., Sun, A. and Altobelli, S. A numerical and experimental study of batch sedimentation and viscous resuspension. *Int. J. Numer. Meth. Fluids*, 39, 465, 2002.

Cook, B. P., Bertozzi, A. L. and A. E. Hosoi. Shock solutions for particle-laden thin films. *SIAM Jnl Applied Math.*, 68(3):160–183, 2007/08.

Zhou, J., Dupuy, B., Bertozzi, A. L. and A. E. Hosoi, Theory for shock dynamics in particle-laden thin films. *Phys. Rev. Lett.*, 94: 117803, 2005.

H. E. Huppert. Flow and instability of a viscous current down a slope. *Nature*, 300:427–429, 1982.

B. P. Cook. Lubrication Models for Particle Laden Thin Films. *PhD–thesis, UCLA CAM Report*, (07–42), 2007.

I. M. Krieger. Rheology of monodisperse lattices. *Adv. in Colloid and Interface Sci.*, 3:111–136, 1972.

Stickel J. J. and R. L. Powell. Fluid mechanics and rheology of dense suspersions. *Ann. Ref. Fluid. Mech.*, 37:129–149, 2005.

G. I. Taylor. Sedimentation and Falling Bodies: Low Reynolds Number Flow. Film, available from http://web.mit.edu/fluids/www/Shapiro/ncfmf.html

Richardson, J. F. and W. N. Zaki, Sedimentation and fluidization: Part I. *Trans. Inst. Chem. Eng.*, 32:35–53, 1954.

Buscall, B., Goodwin, J. W., Ottewill, R. H. and T. F. Tadros. The settling of particles through Newtonian and non-Newtonian media. *J. Colloid and Interface Sci.*, (85):78–86, 1982.

Bertozzi, A. L. and M. Brenner. Linear Stability and Transient Growth in Driven Contact Lines. *Physics of Fluids*, 9(3):530–539, 1997.

Ward, T., Wey, C., Glidden, R., Hosoi, A. E. and A. L. Bertozzi. Experimental study of gravitation effects on the effective shear viscosity of a particle-laden thin film on an inclined plane. *submitted Physics of Fluids*, 2008.

P. D. Lax. Hyperbolic systems of conservation laws and mathematical theory of shock waves. *CBMS-NSF Regional Conference Series in Applied Mathematics, SIAM*, 11, 1973.

L. C. Evans. Partial Differential Equations. *American Mathematical Society*, 1998.

Kranzer, H. C. and B. L. Keyfitz, A strictly hyperbolic system of conservation laws admitting singular shocks. *IMA Volumes in Mathematics and its Applications*, 27:107–125, 1990.

Benjamin Cook, Oleg Alexandrov, and Andrea Bertozzi, Linear stability and nonlinear dynamics in particle laden thin films, *European Physical Journal*, to appear 2009.

D. Leighton and A. Acrivos. The shear induced migration of particles in concentration suspensions. *Chem. Engng. Sci.* 41 1377 (1986).

D. Leighton and A. Acrivos. The shear-induced migration of particles in a concentration suspension. *J. Fluid Mech.*, 181, 415 (1987).

Benjamin P. Cook, Theory for particle settling and shear-induced migration in thin-film liquid flow, *Phys. Rev. E* 78, 045303 (2008).